ELSEVIER

Chemical Engineering Journal 84 (2001) 525–531

Chemical Engineering Journal

www.elsevier.com/locate/cej

Modelling of catalytically stabilised thermal combustion of chlorinated hydrocarbons

Davide Fissore, Antonello A. Barresi*

Dipartimento di Scienza dei Materiali ed Ingegneria Chimica, Politecnico di Torino,
Corso Duca degli Abruzzi 24, 10129 Torino, Italy

Received 16 August 2000; accepted 3 January 2001

Abstract

The combustion of lean mixtures of chloromethane in thermally and catalytically stabilised thermal reactors is considered in this paper. A plug flow model is adopted, with detailed kinetics for homogeneous combustion; mass transfer limitations to the reactive wall are considered, and the influence of gas phase reactions on mass transport coefficients is taken into consideration. The numerical investigation evidenced that the final product distribution is very sensitive to the scheme of heterogeneous reactions considered. By means of a sensitivity analysis, a reduced lumped mechanism is proposed for the reactions at the catalytic wall which is able to describe the experimental data.

Keywords: Plug flow model; Thermally and catalytically stabilised thermal combustion; Reduced lumped mechanism

1. Introduction

Thermally and catalytically stabilised thermal combustors have been proved to be a suitable technology for the complete combustion of lean mixtures containing chlorinated hydrocarbons: very low emissions can be obtained with very short residence time [1–4]. The role of the catalyst has been shown to be important, influencing both conversion and product distribution [4]. The active catalytic surface can provide heat and reactive species to the gas phase, thus extending the region of flame stability beyond the lean region. This is particularly important in chlorinated hydrocarbons combustion, where the chlorinated radicals react with $H^\bullet$, reducing $OH^\bullet$ formation and so inhibiting one of the main chain branching steps [5]. The reactor wall can play an important role even in absence of catalyst: due to its thermal inertia, it sustains the homogeneous combustion, preventing its extinction at low stoichiometric ratio, but can also act as a sink for the radical species [1,6,7].

The understanding of the interactions between the wall and the gas phase is still limited. Driscoll et al. [8], considering the oxidation of H_2 over polycrystalline Pt, showed that $OH^\bullet$ radicals were desorbed from catalyst surface at low pressures; these studies were confirmed by Hellsing et al. [9] who also considered different O_2/H_2 ratios. Ljungstrom et al. [10] compared the activation energy for $OH^\bullet$ desorption from different catalysts (Pt, Pd, Rh, ...) during H_2 oxidation. Interesting data of generation and desorption of $OH^\bullet$ over Pt at low and atmospheric pressure for a great variety of fuel-air mixtures (H_2, CH_4, C_2H_2, C_2H_4) were reported by Griffin et al. [11,12].

The relevance of the contribution of $OH^\bullet$ surface generation has been evidenced by the modelling work of Markatou et al. [13,14], who considered the enhancement of gas phase CH_4 and H_2 oxidation due to the surface generation of $OH^\bullet$ over a Pt-based catalyst. On the other hand Vlachos [15] reported the results of a sensitivity analysis, which evidenced that $OH^\bullet$ desorption from Pt in hydrogen combustion has a negligible influence on the homogeneous reaction: this is a consequence of the high activation energy for the radical desorption, higher than that of the surface reactions. He also considered the possibility of the catalyst acting as a sink of radical, evaluating the influence of several reaction steps on the ignition temperature.

The desorption of $O^\bullet$ during the oxidation of methane at lean equivalence ratio over a platinum and a quartz surface has been measured by Pfefferle and Griffin [16]. Alkylic radicals ($CH_3^\bullet$, ...) have been supposed to desorb from Al_2O_3, SiO_2 and MgO during the combustion of CH_4 at low pressure. The possible relevance of the contribution of these species has been pointed out by Goralski and Schmidt

---

* Corresponding author. Tel.: +39-011-5644658; fax: +39-011-5644699.
E-mail address: barresi@athena.polito.it (A.A. Barresi).

1385-8947/01/$ – see front matter © 2001 Elsevier Science B.V. All rights reserved.
PII: S1385-8947(01)00125-5

Nomenclature

c_i	concentration in the gas phase ($\mathrm{mol\,m^{-3}}$)
$c_{i,\mathrm{s}}$	concentration on the catalytic surface ($\mathrm{mol\,m^{-3}}$)
D	reactor diameter (m)
D_i	molecular diffusivity ($\mathrm{m^2\,s^{-1}}$)
$Da_{i,\mathrm{g}}$	Damköler number for gas phase reaction
$Da_{i,\mathrm{s}}$	Damköler number for surface reactions
F	corrective factor for mass transfer coefficient
k_c	pseudo-first order kinetic constant ($\mathrm{m\,s^{-1}}$)
$k_{i,\mathrm{g}}$	mass transfer coefficient ($\mathrm{m\,s^{-1}}$)
$k_{i,\mathrm{s}}$	kinetic constant for surface reaction ($\mathrm{s^{-1}\,m^2_{cat}\,m^3_{reac}}$)
R_i	net generation rate in the gas phase ($\mathrm{mol\,m^{-3}\,s^{-1}}$)
$R_{i,\mathrm{s}}$	net generation rate on the catalytic surface ($\mathrm{mol\,m^{-2}\,s^{-1}}$)
Sh_i	Sherwood number
Sh_∞	asymptotic Sherwood number (heterogeneous reactions only)
Sh'_∞	asymptotic Sherwood number (corrected for homogeneous reactions)
T	temperature (K)
v_g	gas velocity ($\mathrm{m\,s^{-1}}$)
z	axial coordinate (m)
Greek letter	
η	conversion

[17], but up to now it has not been taken into account in any modelling work; as concern the desorption/recombination of chlorinated radicals over catalytic or non-catalytic surfaces, no data are available.

Both monodimensional and bidimensional models can be used to design these systems: the former are much simpler as they neglect radial gradients, but heat and mass transport to the wall must be properly modelled; the latter are more time consuming and have been used only for very simple systems (see for example [18]). A complete review of the model alternatives can be found in Pfefferle [19]. Recently, Goralski and Schmidt [17] considered the heterogeneous/homogeneous reactions in the high temperature catalytic combustion of methane, using a monodimensional model, but without taking into consideration mass transfer limitations.

Our aim is to use a simple monodimensional model, which takes into consideration mass transfer to the wall, to describe the combustion of lean mixtures of CH_3Cl in air in the catalytically stabilised reactor, in order to explain how the catalytic surface sustains the homogeneous combustion. The noncatalytic case will be considered for comparison and to validate the gas-phase reaction mechanism. Experimental results published in previous works [4,20] will be considered to validate our model.

2. The model

The combustion of lean mixtures of CH_3Cl in air (equivalence ratio = 0.03, corresponding to 5000 ppm by volume), in a small diameter (1.6 mm i.d.) isothermal tubular reactor will be considered. The same conditions used by Hung and co-workers [4,20] will be adopted, in order to use their experimental results to validate the modelling results. The reactor walls can be coated by a manganese oxide or platinum catalyst; the cold flow gas velocity (at 20°C and 100 kPa) is $1.7\,\mathrm{m\,s^{-1}}$, and in the reacting section the velocity profile is fully developed. Further details on the experimental set-up are given in [4].

A plug flow model with isobaric conditions is adopted; the temperature is fixed according to the experimental measurements and is kept constant all the reactor length [4]. Radial convection is neglected and radial diffusion in the balance equations is described by a flux at the wall estimated by the product of the transfer coefficient and a linear driving force between the bulk and the wall.

The mass balance for the *i*th species in the gas phase is

$$v_\mathrm{g}\frac{\mathrm{d}c_i}{\mathrm{d}z} = R_i - \frac{4k_{i,\mathrm{g}}}{D}(c_i - c_{i,\mathrm{s}}) \tag{1}$$

while on the catalyst surface we have

$$-k_{i,\mathrm{g}}(c_i - c_{i,\mathrm{s}}) = R_{i,\mathrm{s}} \tag{2}$$

where R_i and $R_{i,\mathrm{s}}$ are the net generation rate in the gas phase and at the surface respectively.

In the catalytically stabilised combustion reactor, the exothermic surface reactions sustain the homogeneous combustion, but the role of the catalyst is much more complex, as the wall can act as a source or a sink of free radicals, modifying the ignition characteristics and the combustion distribution products of the fuel-air mixture considered.

In laminar flow the transport coefficients in presence of a wall reaction can be evaluated [21–23]. Tronconi and Forzatti [21] showed the dependence of the asymptotic Sherwood number (Sh_∞) on the Damköler number of the surface reactions ($Da_{i,\mathrm{s}}$) for an isothermal reactor, with first order surface reactions and different channel geometry.

When homogeneous reactions occur in the gas phase, the concentration profiles will be distorted, increasing or decreasing the diffusional flux at the wall. For this case a correction factor F can be introduced such that:

$$Sh_\infty = F\,Sh_\infty \tag{3}$$

F depends primarily on the Damköler number for the gas phase, $Da_{i,\mathrm{g}}$, which is the ratio of predominant transport and reaction time scales for reactive species [24]. For the case of a first-order reaction which is a sink for the diffusing species

$$F = \frac{(Da_{i,\mathrm{g}})^{1/2}}{\sinh((Da_{i,\mathrm{g}})^{1/2})} \tag{4}$$

while if the species is generated

$$F = \frac{(Da_{i,\mathrm{g}})^{1/2}}{\sin((Da_{i,\mathrm{g}})^{1/2})} \tag{5}$$

In the case of a first (or pseudo-first order) reaction, the concentration on the catalyst can be easily related to the bulk concentration and Eq. (1) reduces to

$$v_\mathrm{g}\frac{\mathrm{d}c_i}{\mathrm{d}z} = R_i - \frac{4}{D}k_\mathrm{c}c_i \tag{6}$$

where the pseudo-first order kinetic constant:

$$k_\mathrm{c} = \left(\frac{1}{k_{i,\mathrm{g}}} + \frac{1}{k_{i,\mathrm{s}}}\right)^{-1} \tag{7}$$

The decomposition reactions are first order; for the other reactions, as a first approach, the pseudo-first order approximation will be adopted, considering that one reactant is in large excess (O_2) or can be assumed in pseudo-steady state (chlorinated or hydrocarbon radicals). From the definitions of $k_{i,\mathrm{g}}$ and $Da_{i,\mathrm{s}}$

$$k_{i,\mathrm{g}} = \frac{D_i\, Sh_i}{D}, \qquad Da_{i,\mathrm{s}} = \frac{k_{i,\mathrm{s}}D}{D_i} \tag{8}$$

it follows that in case of kinetic control

$$F\,Sh \gg Da_{i,\mathrm{s}} \tag{9}$$

while for diffusive control the opposite holds:

$$F\,Sh \ll Da_{i,\mathrm{s}} \tag{10}$$

As shown above $F = F(Da_{i,\mathrm{g}})$, while $Sh = Sh(Da_{i,\mathrm{s}})$. When the component is generated by the homogeneous reactions, the higher is $Da_{i,\mathrm{g}}$ the higher is the correction factor of the mass transfer coefficient (F): kinetic control occurs generally in this case, unless the surface reactions are extremely fast. If the component is depleted in the gas phase, the higher is $Da_{i,\mathrm{g}}$ the lower is F; in this case, we are under diffusive control unless the surface reactions are very slow.

We can plot the previous expressions and use the obtained chart to verify if a reaction is under diffusive or kinetic control. $Da_{i,\mathrm{s}}$ is easy to calculate from the kinetic scheme employed to describe surface processes, while F can be determined from the contribution of the homogeneous reactions to overall conversion.

A detailed kinetic model including elementary reactions is adopted to describe the evolution of the reacting species, comparing the reaction schemes proposed by different authors (see Section 3.1). The thermodynamic data reported by each author have been used for computations; the adopted model use the same data of Hung and Pfefferle [20].

A code has been realised in MATLab environment, employing a multistep solver, with variable order, based on the numerical differentiation formulas (ode15s), to solve the system of stiff ordinary differential equations (ODE) which arises from the mass balance. The stiffness of the problem arises from the kinetic constants of the radical reactions considered, which can be of very different magnitude order.

In order to identify the main homogeneous reactions playing a role in gas phase in absence of catalyst and the main reaction paths, a sensitivity analysis of the homogeneous reaction scheme has been carried out. The method of principal component analysis of concentration sensitivity matrices has been adopted [25], using the package KINAL [26].

The results of the sensitivity analysis have been also used to select the more relevant reactions on the catalytic surface; lumped reaction schemes have been also adopted to model the surface reactions in the catalytically stabilised reactor.

The kinetic parameters at each temperature have been determined by best fitting with the experimental data using the minimum square method; the confidence interval for the estimated parameters is in the range ±1–5%.

3. Results and discussion

3.1. Combustion of lean CH_3Cl mixtures in the non-catalytic reactor

Several models have been proposed for the thermal combustion of mixtures of CH_3Cl in air. Ho et al. [27] considered 66 reacting species and 194 reactions; the model was developed to fit methyl chloride, intermediates and final products species at different temperatures and reaction times, but for high values of the equivalence ratio. There are two different versions of the model, according to two different methods used to find the kinetic constants of some bimolecular reactions; both models show a poor agreement with the data of Hung et al. [4], which were obtained burning a lean mixture. The model of Karra et al. [28] was developed for freely propagating flames and considers 87 species and 185 reactions; also in this case the agreement with the experimental data is poor (see Fig. 1).

A better agreement is obtained with the model proposed by Hung and Pfefferle [20], which is derived from that of Karra et al.; some kinetic parameters have been modified and

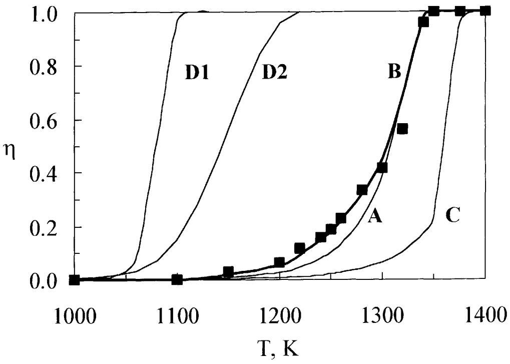

Fig. 1. CH_3Cl conversion in the noncatalytic reactor; comparison of experimental data (■) (from [20]) with the predictions of the model by (A) Hung and Pfefferle [20]; (B) Hung and Pfefferle modified (this work); (C) Karra et al. [28]; (D1) Ho et al. [27] (base version) and (D2) Ho et al. [27] (using DISSOC).

new reaction paths are considered, for example, the recombination of $CH_2Cl^\bullet$ and $CH_3^\bullet$ to origin C_2 species before the oxidation.

It must be evident that the influence of the small diameter and the wall effects on the kinetic parameters are probably relevant, but these have been implicitly taken into account: in fact, the kinetic parameters of the model proposed by Hung and Pfefferle were optimised by them to fit a set of experimental data of fuel-lean oxidation of CH_3Cl in conditions very similar to those used in this work. The previous model can be further improved: the kinetic constants of two reactions of the new paths introduced by Hung and Pfefferle [20] ($1,2\text{-}C_2H_4Cl_2 \leftrightarrow 2CH_2Cl^\bullet$ and $C_2H_5Cl \leftrightarrow CH_3^\bullet + CH_2Cl^\bullet$) can be modified, by estimating the kinetics parameters of the reverse reactions from the value of the equilibrium constant, similarly to what done for other reversible reactions. A very good agreement with the experimental data is obtained, as shown in Fig. 1.

The sensitivity analysis realised with KINAL points out that at the beginning the most important reactions are the decomposition of CH_3Cl and O_2:

$$CH_3Cl \rightarrow CH_3^\bullet + Cl^\bullet \tag{11}$$

$$O_2 \rightarrow 2O^\bullet \tag{12}$$

and the oxidation of CH_3Cl

$$CH_3Cl + O_2 \rightarrow CH_2Cl^\bullet + HO_2^\bullet \tag{13}$$

After these initial steps, the recombination of the radical originates the products of complete and incomplete oxidation; CO is mainly produced by the oxidation of CHO:

$$CHO + O_2 \rightarrow CO + HO_2^\bullet$$

and destroyed by $CH_2^\bullet$:

$$CO + CH_2^\bullet \rightarrow C_2H_2O \tag{15}$$

The oxidation of CH_2 is also the main path for the production of CO_2:

$$CH_2^{\bullet\bullet} + O_2 \rightarrow CO_2 + 2H^\bullet \tag{16}$$

The recombination of $CH_3^\bullet$ is the main path to obtain C_2H_2, C_2H_4 and C_2H_6:

$$CH_3^\bullet + CH_3^\bullet \rightarrow C_2H_2 + 2H_2 \tag{17}$$

$$CH_3^\bullet + CH_3^\bullet \rightarrow C_2H_4 + H_2 \tag{18}$$

$$CH_3^\bullet + CH_3^\bullet \rightarrow C_2H_6 \tag{19}$$

The recombination of $CH_2Cl^\bullet$ leads to the other main products of combustion:

$$CH_2Cl^\bullet + CH_2Cl^\bullet \rightarrow C_2H_3Cl + HCl \tag{20}$$

$$CH_2Cl^\bullet + CH_2Cl^\bullet \rightarrow 1,2\text{-}C_2H_4Cl_2 \tag{21}$$

3.2. Combustion of lean CH_3Cl mixtures in the catalytically stabilised reactor

The definition of the kinetic scheme for the surface reactions both on the Mn-based and on the Pt catalyst is a problem with a high number of degrees of freedom, as we have no direct experimental information about the species involved, the reactions which take place and their kinetic parameters. The aim of this work has not been to point out all the elementary reactions which can take place on the surface, but to find a simple kinetic scheme which can account for the experimental results, in order to point out the role of the catalyst in sustaining the homogeneous reactions. Thus, the contribution of the catalyst to the main gas phase reactions evidenced from the sensitivity analysis has been taken into consideration. The catalyst surface is considered in steady state.

3.2.1. Manganese oxide catalyst

The minimum scheme of surface reactions required to describe the catalytically stabilised combustion of lean mixtures of methyl chloride in air over a Mn-based catalyst is given below; it considers both decomposition and recombination reactions:

$$CH_3Cl \rightarrow CH_3^\bullet + Cl^\bullet \tag{A1}$$

$$CH_3^\bullet + CH_3^\bullet \rightarrow C_2H_2 + 2H_2 \tag{A2}$$

$$CH_3^\bullet + CH_3^\bullet \rightarrow C_2H_4 + H_2 \tag{A3}$$

$$CH_3^\bullet + CH_3^\bullet \rightarrow C_2H_6 \tag{A4}$$

$$CH_2Cl^\bullet + O_2 \rightarrow CH_2O + ClO^\bullet \tag{A5}$$

As the main reaction in the homogeneous combustion is the decomposition of CH_3Cl into $CH_3^\bullet$ and $Cl^\bullet$ (reaction A1), and the catalyst enhances conversion, we have considered that this reaction takes place also on the surface. Similarly, as the production of C_2H_2, C_2H_4 and C_2H_6 pass through the recombination of $CH_3^\bullet$, we have assumed that the methyl radicals can recombine also on the catalyst to give different C_2 products (reactions A2, A3, A4). The ratio CO/CO_2 can be controlled through the intermediates CH_2O and ClO (reaction A5). Fig. 2 shows the temperature dependence of the pseudo first-order kinetic constants k_c: decomposition of CH_3Cl and oxidation of chlorinated radicals seem to be under diffusion control, while the methyl radical recombination reactions seem to be under kinetic control. These considerations are confirmed by the criterion we have previously described, as we can see from Fig. 3.

Fig. 4 show the comparison between the experimental data and the distribution of combustion products predicted by our model. The agreement is generally very satisfactory; only the ethene formation is slightly overestimated.

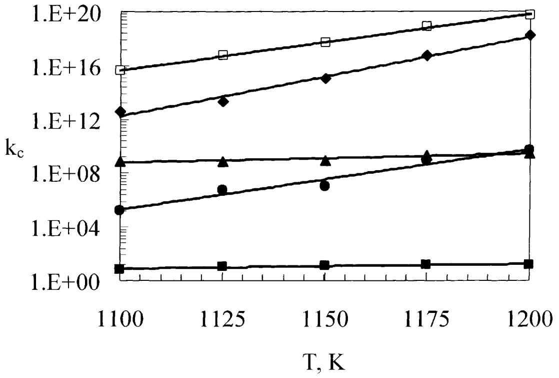

Fig. 2. Temperature dependence of the pseudo-first-order kinetic constants of the surface reactions over the Mn-based catalyst: reactions A1 (■), A2 (●), A3 (◆), A4 (□), A5 (▲). The points represent the values obtained by best fitting at each temperature, connected by trendlines.

3.2.2. Pt-based catalyst

Platinum is a very effective oxidation catalyst; thus the contribution of surface oxidation reactions to total conversion is significant, but differently from the previous case, the depletion reactions prevail over the radical generation. This is demonstrated by the fact that the temperature required for complete conversion is slightly higher than in the case with no catalyst, but the production of PIC is much lower.

The catalytically stabilised combustion of lean methyl chloride in air over a Pt-based catalyst can be modelled including the following kinetic scheme for the surface reactions:

$$CH_3Cl + 2O_2 \rightarrow CO_2 + H_2O + HOCl \tag{B1}$$

$$CH_2Cl^{\bullet} + O_2 \rightarrow CH_2O + ClO^{\bullet} \tag{B2}$$

$$2CO + O_2 \rightarrow 2CO_2 \tag{B3}$$

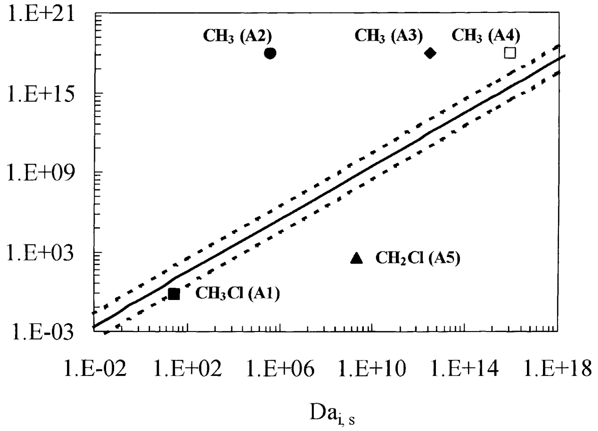

Fig. 3. Evaluation of the reaction regime for the wall reactions over the Mn-based catalyst at the temperature of 1100 K. The dashed lines correspond to $F\,Sh = 10\,Da_{i,s}$ (Eq. (9)) and $F\,Sh = 0.1\,Da_{i,s}$ (Eq. (10)); symbols as in Fig. 2.

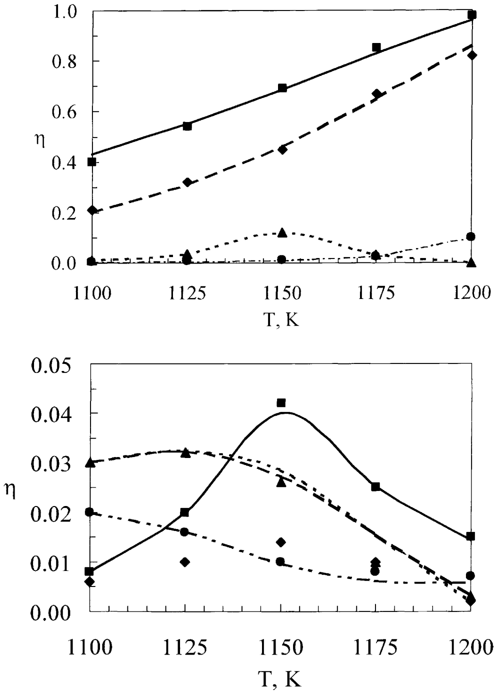

Fig. 4. Comparison between experimental and predicted values for the conversion of CH_3Cl over the Mn-based catalyst. Upper graph: total CH_3Cl conversion (—,■); conversion to CO (———,◆); to CO_2 (———,●); to CH_4 (× 10) (– – – –,▲). Lower graph: conversion to C_2H_2 (—, ■); to C_2H_4 (– – – –,◆); to C_2H_6 (————,●); to C_2H_3Cl (————,▲).

The decomposition of CH_3Cl into $CH_3^{\bullet}$ and $Cl^{\bullet}$ and the decomposition of O_2 into $O^{\bullet}$, which are the most important reactions in the homogeneous combustion, are lumped in reaction B1. To fit the experimental distribution of C_2 products it is necessary to introduce a surface reaction which oxidises chlorinated radicals before their gas-phase recombination (reaction B2), while the CO/CO_2 ratio is controlled through reaction B3. Fig. 5 shows the temperature dependence of the kinetic constants: the oxidation of CH_3Cl and chlorinated radicals is under diffusive control, while the

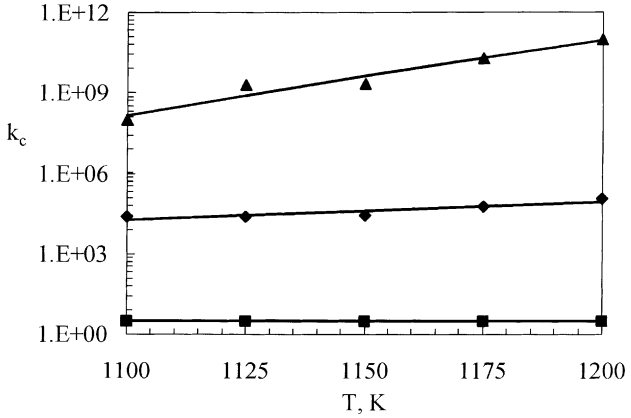

Fig. 5. Temperature dependence of the pseudo-first-order kinetic constants for the surface reactions over the Pt-based catalyst: reactions B1 (■), B2 (◆), B3 (▲).

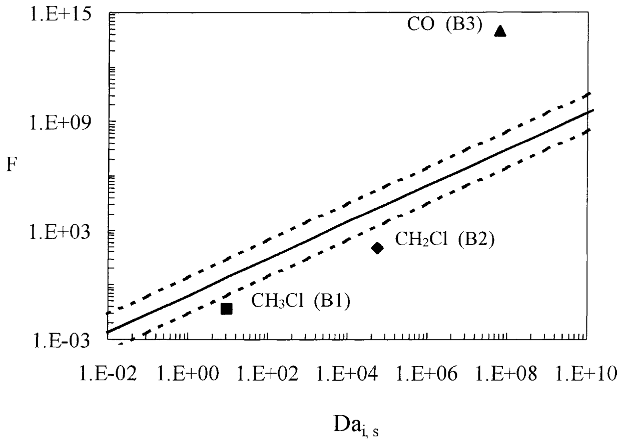

Fig. 6. Evaluation of the reaction regime for the wall reactions over the Pt-based catalyst at the temperature of 1100 K. Symbols as in Fig. 5.

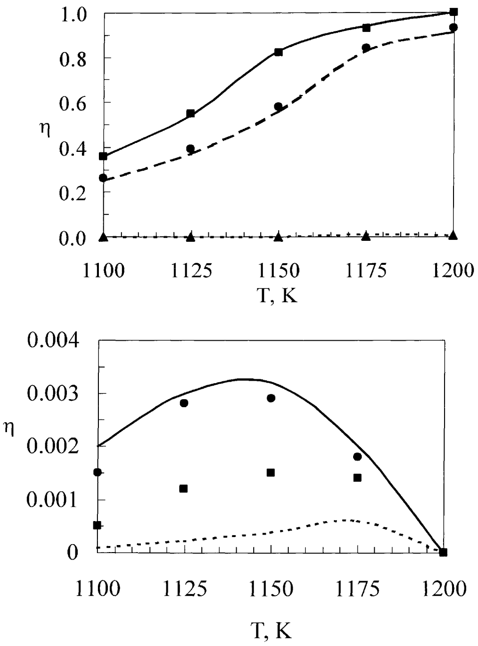

Fig. 7. Comparison between experimental and predicted values for the conversion of CH_3Cl over the Pt-based catalyst. Upper graph: total conversion(—,■); conversion to CO (– – – –,▲); to CO_2 (——— ,●). Lower graph: conversion to C_2H_3Cl (—, ■); to $C_2H_4Cl_2$ (– – – –,●).

oxidation of CO is under kinetic control, as we can see from Fig. 6.

Fig. 7 shows the comparison between the experimental data and the distribution of combustion products predicted by the proposed model. Again the agreement is satisfactory, except for an underprediction of $C_2H_4Cl_2$ formation.

4. Conclusions

The definition of a kinetic scheme for the surface reactions which occur in the catalytically stabilised thermal reactor is a problem with a high number of degrees of freedom as very little information is available about the species involved and the reactions which take place.

A sensitivity analysis has been carried out to point out the reactions which play the most important role in the generation of the main products in the homogeneous combustion; to fit the experimental data for the catalytically stabilised combustion we have assumed that the catalytic surface contributes to the reactions which have the greatest role in the formation of the combustion products in the homogeneous case.

Through mathematical simulation (monodimensional model) we have proposed a kinetic scheme to describe the combustion of chlorinated hydrocarbons in this short-contact-time reactor, pointing out the role of the catalyst surface: the Mn-based catalyst favours the recombination of C_2 radicals leading to significant amounts of C_2 hydrocarbons, while the Pt-based catalyst promotes the oxidation of radicals and molecular species. We have also taken into consideration the mass transport to the wall and the influence of the homogeneous reactions on the mass transfer coefficient, obtaining a simple model which give a good agreement with the experimental data.

Acknowledgements

This work has been financially supported by the Italian Ministry of University (MURST PRIN — Pollutant emission in turbulent combustion at intermediate and high temperature).

References

[1] W.C. Pfefferle, L.D. Pfefferle, Prog. Energy Combust. Sci. 12 (1986) 25–41.
[2] S.L. Hung, L.D. Pfefferle, J. Washington Academy Sci. 77 (1987) 199–204.
[3] S.L. Hung, L.D. Pfefferle, Environ. Sci. Technol. 23 (1989) 1085–1091.
[4] S.L. Hung, A.A. Barresi, L.D. Pfefferle, in: Proceedings of the 23rd International Symposium on Combustion, Orléans, France, 22–27 July 1990. The Combustion Institute, 1991, pp. 909–915.
[5] A.K. Gupta, Chem. Eng. Commun. 41 (1982) 1–21.
[6] D.G. Vlachos, Combust. Flame 103 (1995) 59–75.
[7] P. Aghalayam, D.G. Vlachos, AIChE J. 44 (1998) 2025–2034.
[8] D.J. Driscoll, K.D. Campbell, J.H. Lunsford, Adv. Catal. 35 (1987) 139–186.
[9] B. Hellsing, B. Kasemo, S. Ljungstrom, A. Rosen, T. Wahnstrom, Surf. Sci. 189/190 (1987) 851–860.
[10] S. Ljungstrom, J. Hall, B. Kasemo, A. Rosen, T. Wahnstrom, J. Catal. 107 (1987) 548–556.
[11] T.A. Griffin, L.D. Pfefferle, M.J. Dyer, D.R. Crosely, Combust. Sci. Technol. 30 (1989) 19–37.
[12] T.A. Griffin, M. Calabrese, L.D. Pfefferle, A. Sappey, R. Copeland, D.R. Crosley, Combust. Flame 90 (1992) 11–33.
[13] P. Markatou, L.D. Pfefferle, M.D. Smooke, Combust. Sci. Technol. 79 (1991) 247–268.
[14] P. Markatou, L.D. Pfefferle, M.D. Smooke, Combust. Flame 84 (1993) 185–201.

[15] D.G. Vlachos, Chem. Eng. Sci. 51 (1996) 2429–2438.
[16] L.D. Pfefferle, T.A. Griffin, Combust. Flame 76 (1989) 339–349.
[17] C.T. Goralski, L.D. Schmidt, Chem. Eng. Sci. 54 (1999) 5791–5807.
[18] P.-A. Bui, D.G. Vlachos, P.R. Westmoreland, Ind. Eng. Chem. Res. 36 (1997) 2558–2567.
[19] L.D. Pfefferle, Catal. Today 26 (1995) 255–265.
[20] S.L. Hung, L.D. Pfefferle, Combust. Sci. Technol. 87 (1992) 91–107.
[21] E. Tronconi, P. Forzatti, AIChE J. 38 (1992) 201–210.
[22] A.A. Barresi, M. Vanni, Ind. Chem. Engr. A 39 (1997) 209–213.
[23] R.E. Hayes, S.T. Kolaczkowski, Catal. Today 47 (1999) 295–303.
[24] D.E. Rosner, Transport Processes in Chemically Reacting Flow Systems. Butterworths, Boston, 1986, pp. 320–322.
[25] S. Vajada, P. Valko, R. Turanyi, Int. J. Chem. Kin. 17 (1985) 55–81.
[26] T. Turanyi, Computers Chem. 14 (1990) 253–254.
[27] W. Ho, Q.R. Yu, J.W. Bozzelli, Combust. Sci. Technol. 85 (1992) 23–63.
[28] S.B. Karra, D. Gutman, S.M. Senkan, Combust. Sci. Technol. 60 (1988) 45–62.